Supplementary materials

Divergent functional porous organic polymers used for low concentration CO_2 fixation

Zhifeng Dai,[+*a] Yuanfei Bao,[+a] Jindong Yuan,[+a] Jinzhong Yao,[b] and Yubing Xiong,[*a]

[a] *Key Laboratory of Surface & Interface Science of Polymer Materials of Zhejiang Province, Department of Chemistry, College of Science, Zhejiang Sci-Tech University, Hangzhou 310018, PR China*

[b] *College of Biological, Chemical Sciences and Engineering, Jiaxing University, Jiaxing 314001, China.*

[+] These authors contribute equal to this work.

Experimental Section

Materials

The typical reagents and substrates including azobisisobutyronitrile (AIBN), bromoacetic acid, 2-bromoethylamine hydrobromide, 2-bromoethanol, ethylene chlorohydrins, and epichlorohydrin were purchased from the Shanghai Aladdin Bio-Chem Technology Co., Ltd. and Beijing InnoChem Science & Technology Co., Ltd. These reagents and substrates were purchased with high purity and used without further purification.

Catalysts Preparation

Synthesis of triphenylphosphine based porous organic polymer (POP-PPh_3). The POP-PPh_3 was synthesized through a radical polymerization method from the vinyl-functionalized triphenylphosphine monomer (v-PPh_3). As a typical run, 1 g of v-PPh_3 was dissolved in 10 mL of THF, followed by addition of 50 mg of AIBN. After maintaining in an autoclave at 100 °C for 24 h, the white powder of POP-PPh_3 was finally obtained after dried and used directly for the next step without further purification (0.99 g, 99.0% yield).

Synthesis of amino functionalized porous organic polymer (POP-PA-NH_2). The polar group functionalized porous organic polymers were synthesized from the phosphonium reaction of triphenylphosphine based polymer POP-PPh_3 with the corresponding functional alkyl bromide. Typically, for the synthesis of POP-PA-NH_2, 300 mg of POP-PPh_3 (0.88 mmol) and 180.6 mg of 2-bromoethylamine hydrobromide (0.88 mmol) were dispersed in 10 mL of toluene with stirring, then the mixture was heated to 110 °C for 48 h under N_2. After cooling to room temperature, the solid was filtered and washed with CH_2Cl_2 for several times. The solid was re-dispersed in 20 mL of triethylamine and stirred for 4 h. Then the triethylamine was removed and the solid was washed with ethyl acetate for several times, and dried under vacuum for 12 h. The product of POP-PA-NH_2 was obtained as orange solid (344.5 mg, 88.8% yield). The weight content of Br^- species was calculated to be 8.3 wt%.

The content of the Br^- species in the porous organic polymers were calculated according to the following equation:

$$w(Br^-) = \frac{m_P - m_S}{M_{PG}} \times M_{Br} \div m_P \times 100\%$$

In which the m_p and m_s represent the amount of the yield products and the substrates used for the phosphonium reaction, respectively. M_{PG} represents the molecular weight of the decorated polar group (PG). M_{Br} represents the atomic weight of the Br^- species.

Synthesis of carboxylic acid functionalized porous organic polymer (POP-PA-COOH). For the synthesis of POP-PA-COOH, 300 mg of POP-PPh_3 (0.88 mmol) and 244.5 mg of bromoacetic acid (1.76 mmol) were dispersed in 10 mL of toluene with stirring, then the mixture was heated to 110 °C for 48 h under N_2. After cooling to room temperature, the solid was filtered and washed with ethyl acetate for several times. After dried under vacuum for 12 h, the product POP-PA-COOH was obtained as orange solid (372.6 mg, 87.7 % yield). The content of Br^- species in the porous organic polymer was calculated to be 11.2 wt% accordingly.

Synthesis of hydroxyl group functionalized porous organic polymer (POP-PA-OH). For the synthesis of POP-PA-OH, the process was similar to the previous polymer, except 220.0 mg of 2-bromoethanol (1.76 mmol) was used. The product POP-PA-OH was obtained as light yellow solid (354.5 mg, 86.4 % yield). The content of Br^- species in the porous organic polymer was calculated to be 9.8 wt% accordingly.

Synthesis of the comparison non-functionalized porous organic polymer (POP-PA-Et). For the synthesis of POP-PA-Et, the process was similar to the previous polymer, except 250 mg of POP-PPh_3 and 240.0 mg of bromoethane (2.2 mmol) was used. The product POP-PA-Et was obtained as light yellow solid (282.8 mg, 85.7 % yield). The content of Br^- species in the porous organic polymer was calculated to be 8.5 wt% accordingly.

Catalytic activity test

Typically, the reactions were conducted in a Schlenk tube with 10 mmol of epoxides and CO_2 were purged with a balloon at 333 K over the various catalysts for 48 h. The reactants and products were determined by ^{1}H NMR spectroscopy. For catalytic evaluation under low CO_2 concentration, 15% CO_2 mixed with 85% N_2 in volume was used and other conditions are the same. For recycling tests, the catalyst was filtered and washed with CH_2Cl_2 for three times, and dried in air. Then, the catalyst was used for the next run without further treatment.

Characterization

Nitrogen sorption isotherms collected at 77 K were measured with a Micromeritics ASAP 2020M systems, and the samples were pre-treated under vacuum at 100 °C for 12 h. The surface areas were calculated by the Brunauer-Emmett-Teller (BET) method. CO_2 sorption isotherms were collected from Micromeritics ASAP2010 at 298 K and 273 K under the pressure of 1 atm CO_2. Before the measurement, the samples were treated under vacuum at 100 °C for 12 h. X-ray Photoelectron Spectroscopy (XPS) spectra were performed on a Thermo ESCALAB 250 with Al Kα irradiation at θ = 90° for X-ray sources, and the binding energies were calibrated using the C1s peak at 284.9 eV. Thermal gravimetric analysis (TGA) experiments were performed on a SDT Q600 V8.2 Build100 thermogravimetric analyzer under N_2 flow. Elemental analysis was carried out in the Vario micro cube Organic Element Analyzer (Elementar, Germany). The scanning electron microscopy (SEM) images of the samples were recorded on a Hitachi SU 1510 apparatus. Transmission electron microscopy (TEM) experiments were performed on a JEM-2100F field emission electron microscope (JEOL, Japan) with an acceleration voltage of 110 kV. ^{1}H NMR spectra were recorded on a Bruker Avance-400 (400 MHz) spectrometer. Chemical shifts were expressed in ppm downfield from TMS at δ=0 ppm. Solid-state cross-polarization magic angle spinning ^{13}C and ^{31}P NMR (CP/MAS NMR) spectra were recorded on a Varian infinity plus 400 M spectrometer equipped with a magic-angle spin probe in a 4-mm ZrO_2 rotor.

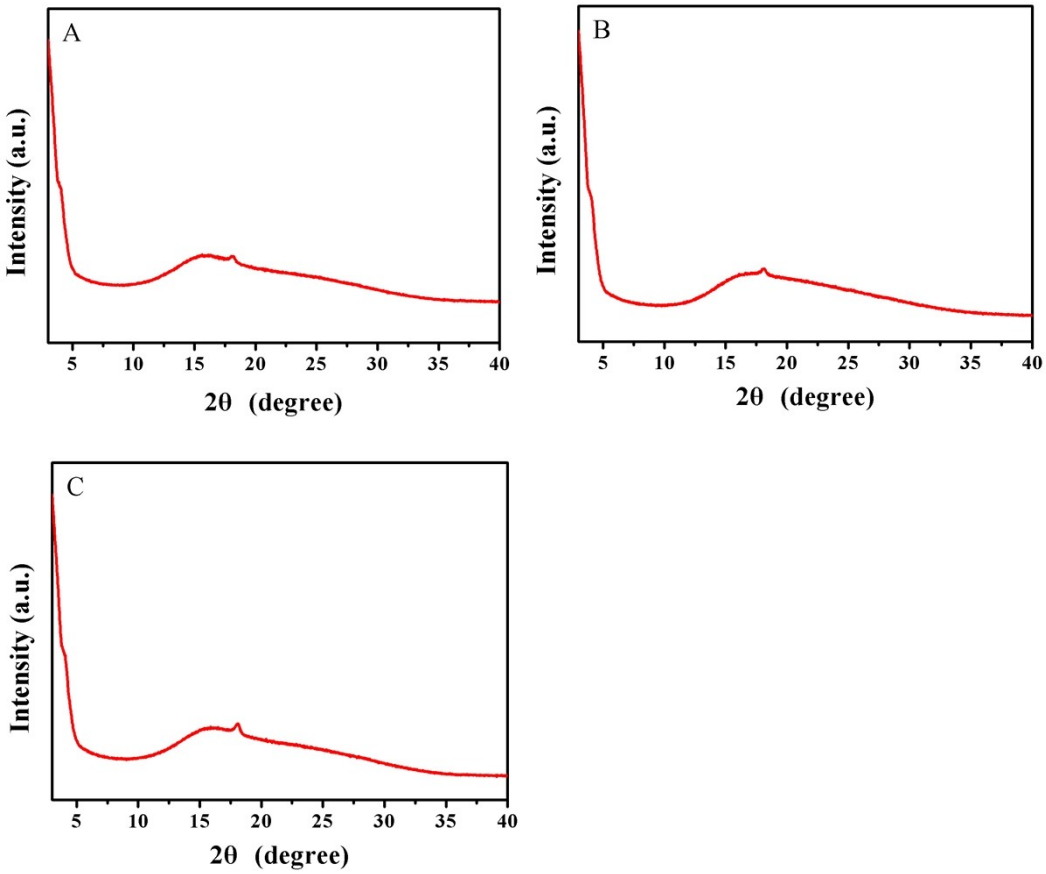

Figure S1. The PXRD spectrum of (A) POP-PA-NH_2, (B) POP-PA-COOH, and (C) POP-PA-OH.

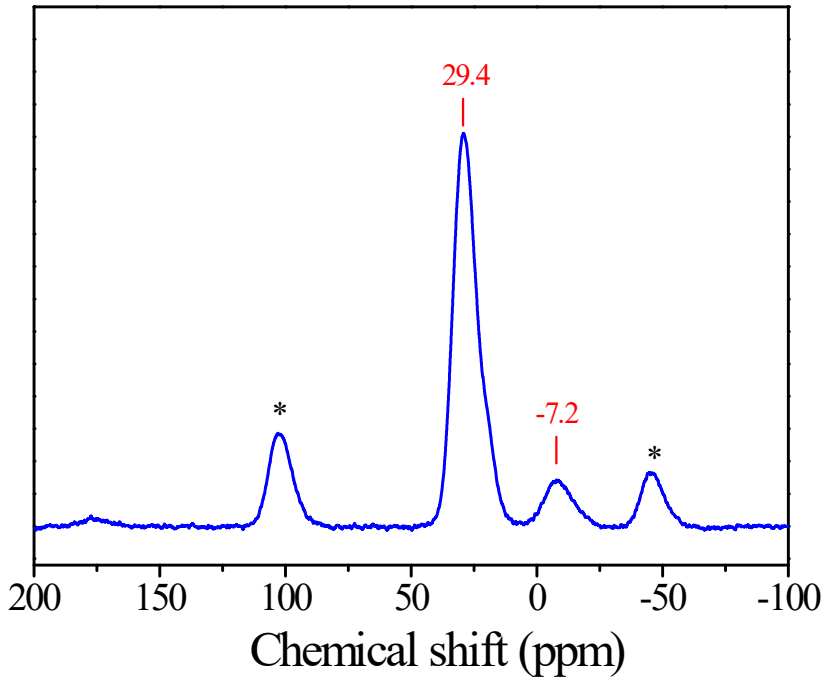

Figure S2. The ^{31}P CP/MAS solid state NMR spectrum of POP-PA-NH_2.

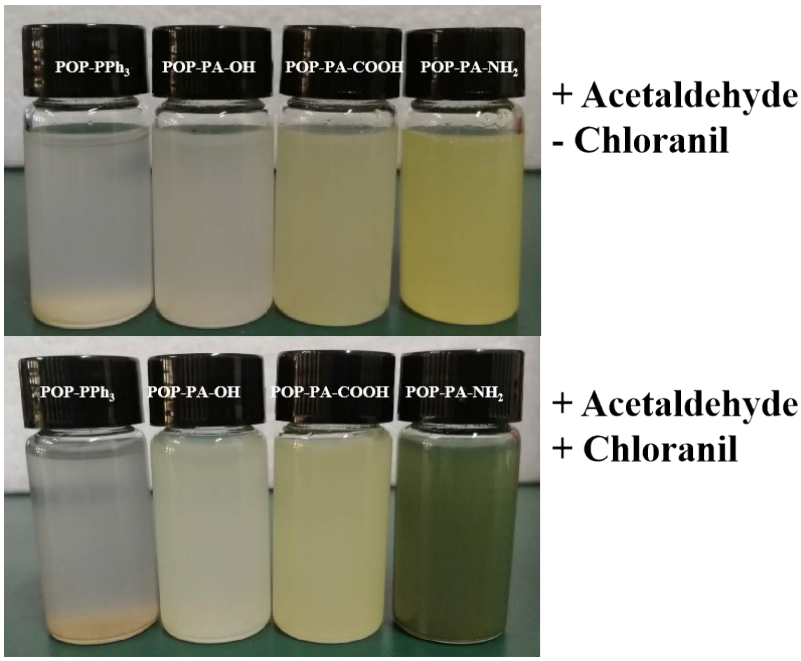

Figure S3. Chloranil test of POP-PPh_3, POP-PA-OH, POP-PA-COOH, POP-PA-NH_2. Only the vial contain polymer POP-PA-NH_2 turns blue-green after the addition of chloranil (5%).

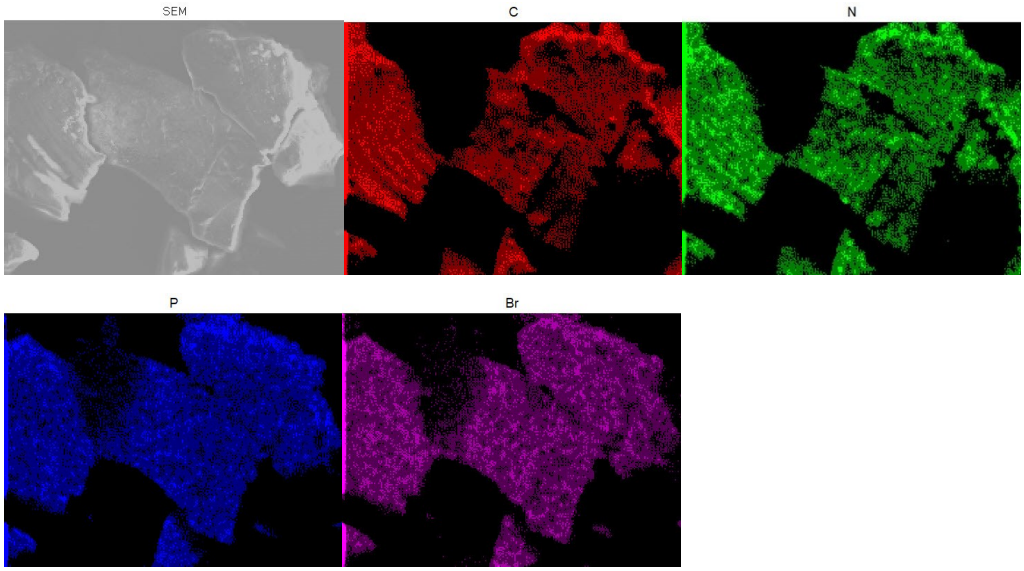

Figure S4. The EDS mapping of POP-PA-NH_2.

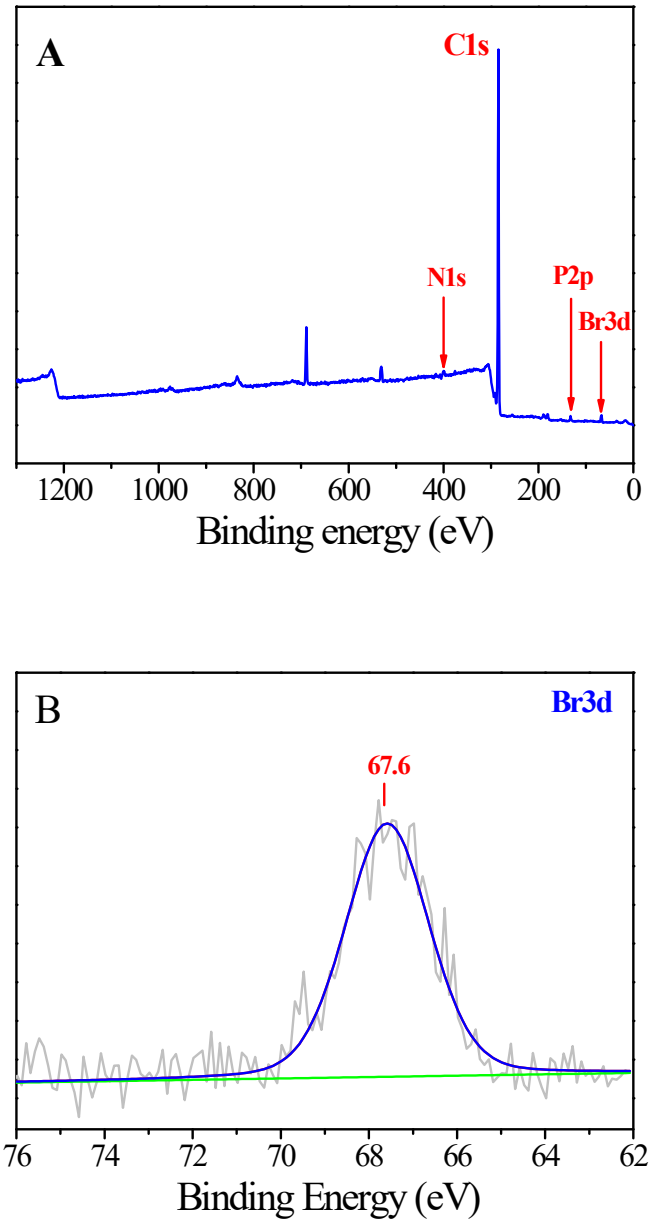

Figure S5. The XPS (A) survey spectrum and (B) Br3d high resolution spectra of POP-PA-NH_2.

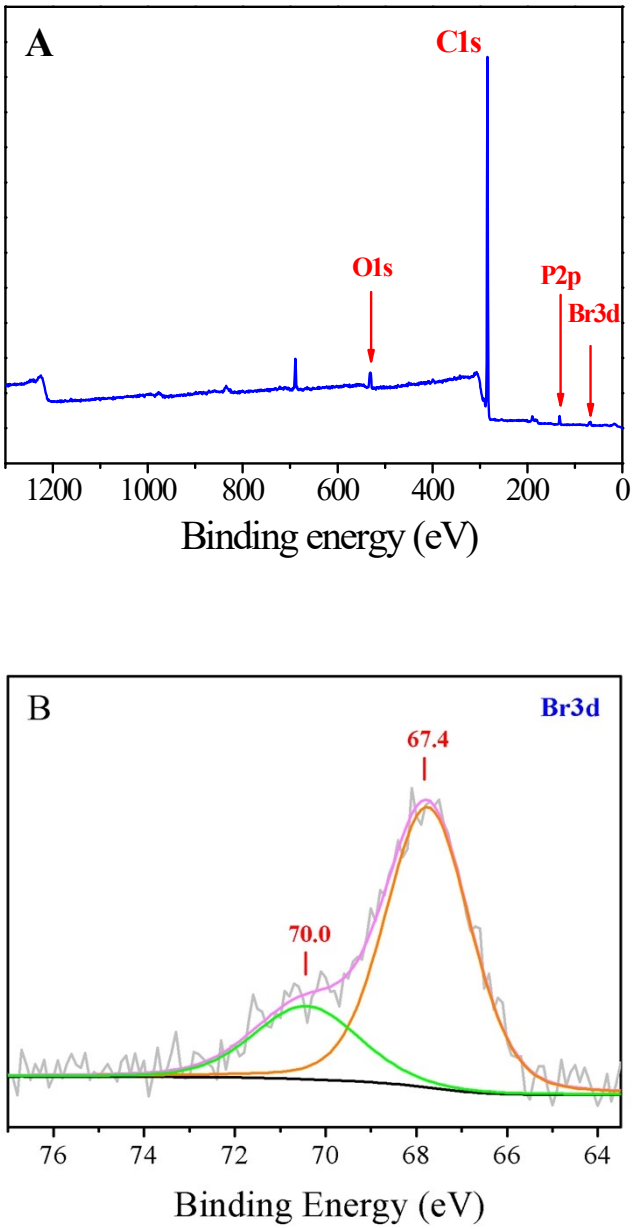

Figure S6. The XPS (A) survey spectrum and (B) Br3d high resolution spectra of POP-PA-COOH.

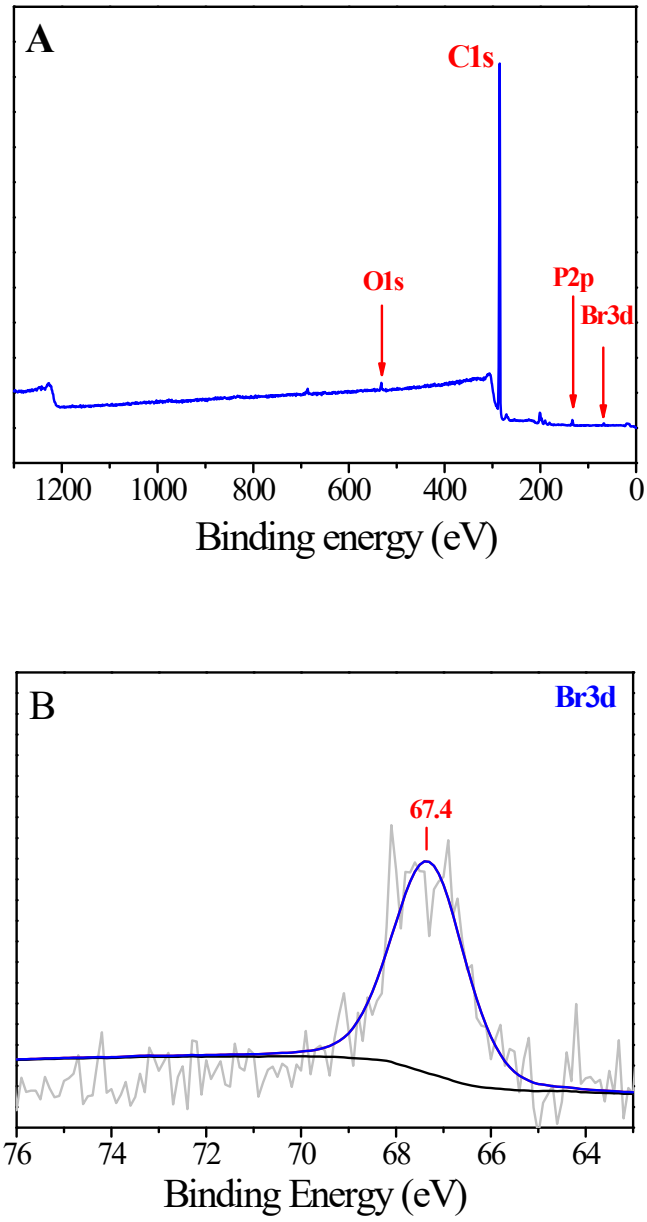

Figure S7. The XPS (A) survey spectrum and (B) Br3d high resolution spectra of POP-PA-OH.

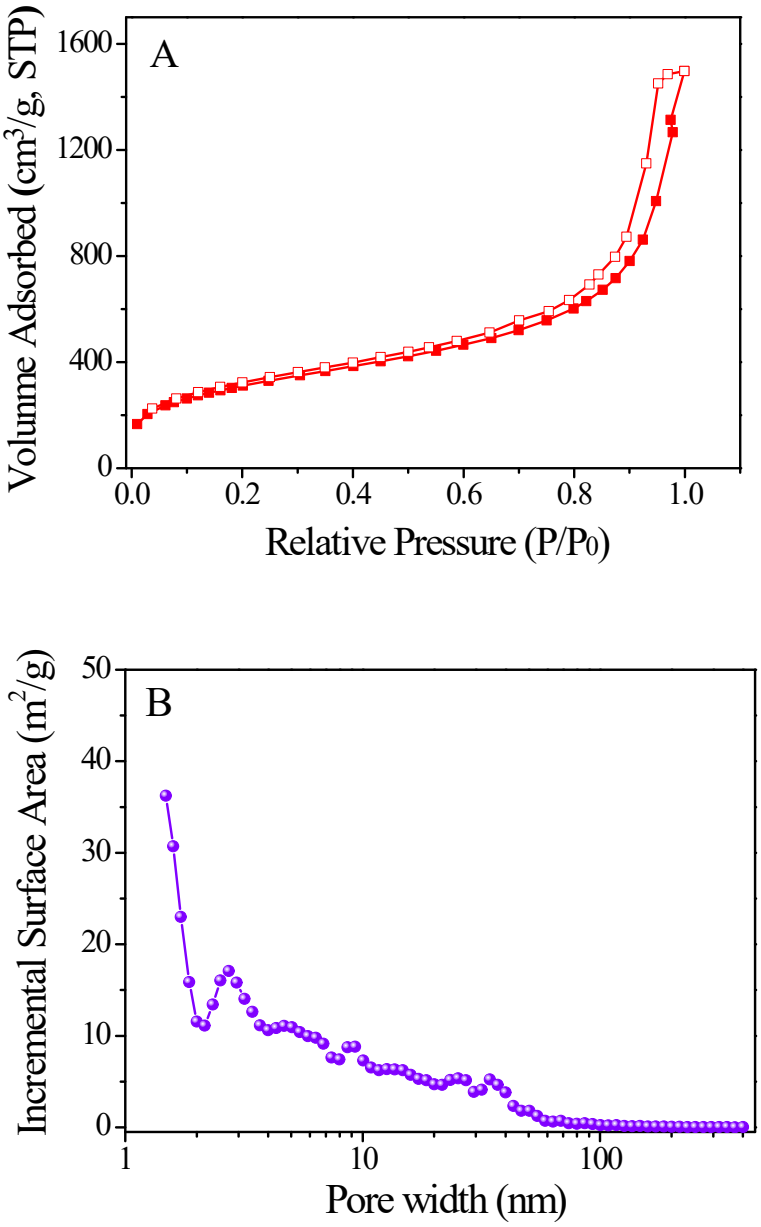

Figure S8. (A) N_2 sorption isotherms and (B) Pore size distribution of POP-PPh_3. The BET surface area and pore volume of them were listed in table S1.

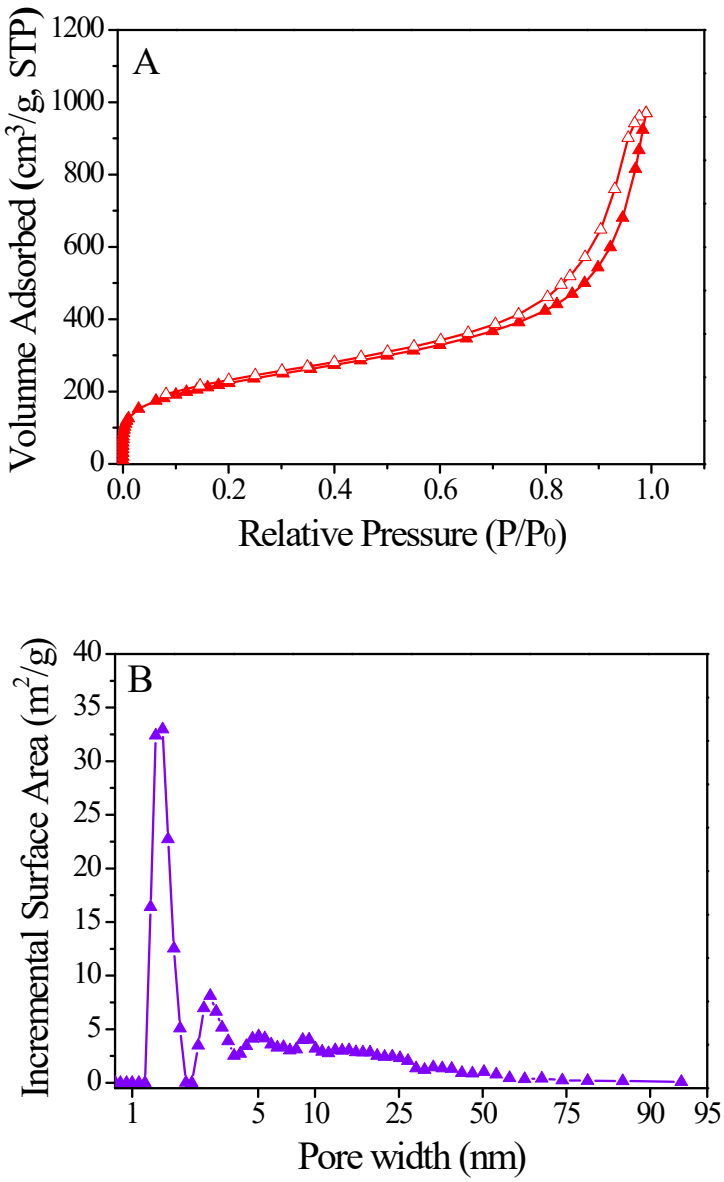

Figure S9. (A) N_2 sorption isotherms and (B) Pore size distribution of POP-PA-COOH. The BET surface area and pore volume of them were listed in table S1.

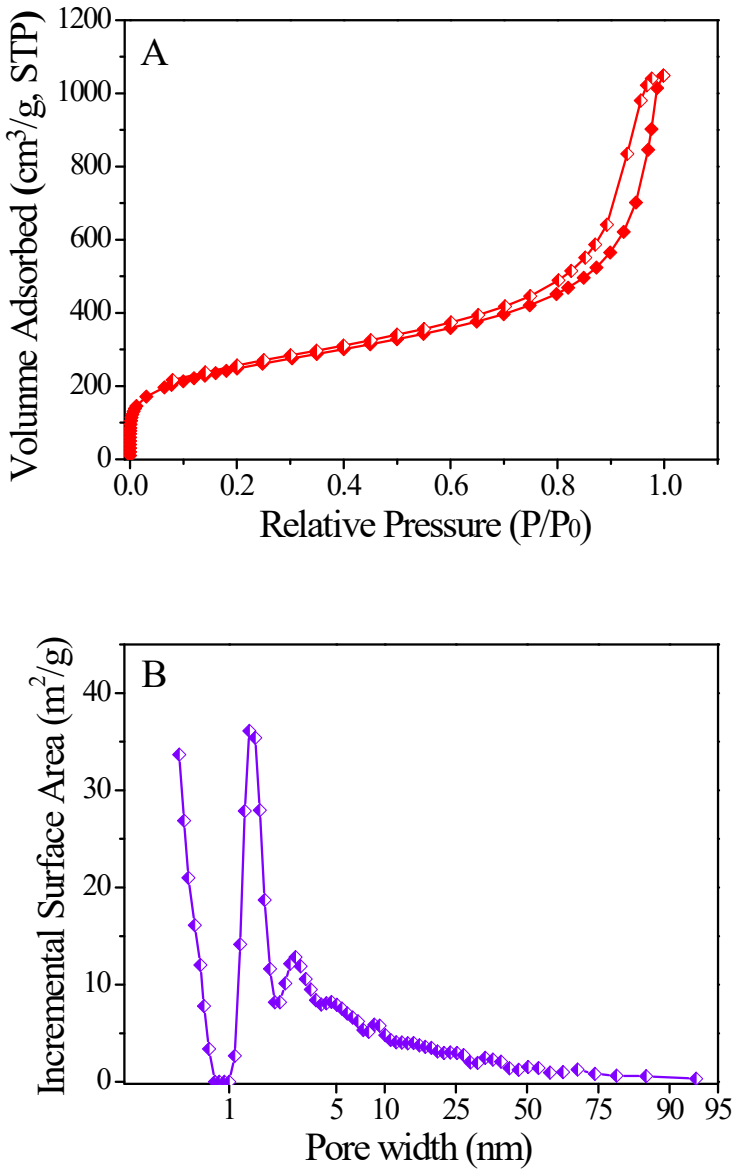

Figure S10. (A) N_2 sorption isotherms and (B) Pore size distribution of POP-PA-OH. The BET surface area and pore volume of them were listed in table S1.

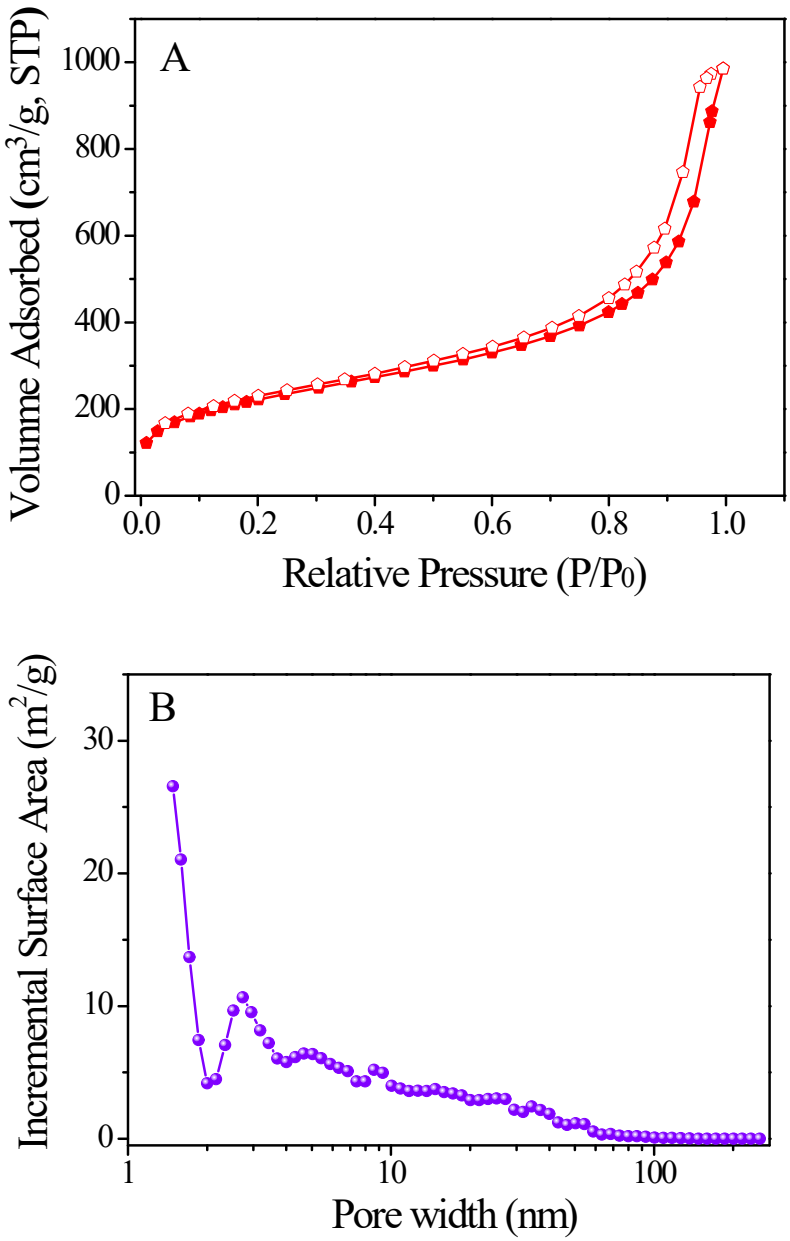

Figure S11. (A) N_2 sorption isotherms and (B) Pore size distribution of POP-PA-Et. The BET surface area and pore volume of them were listed in table S1.

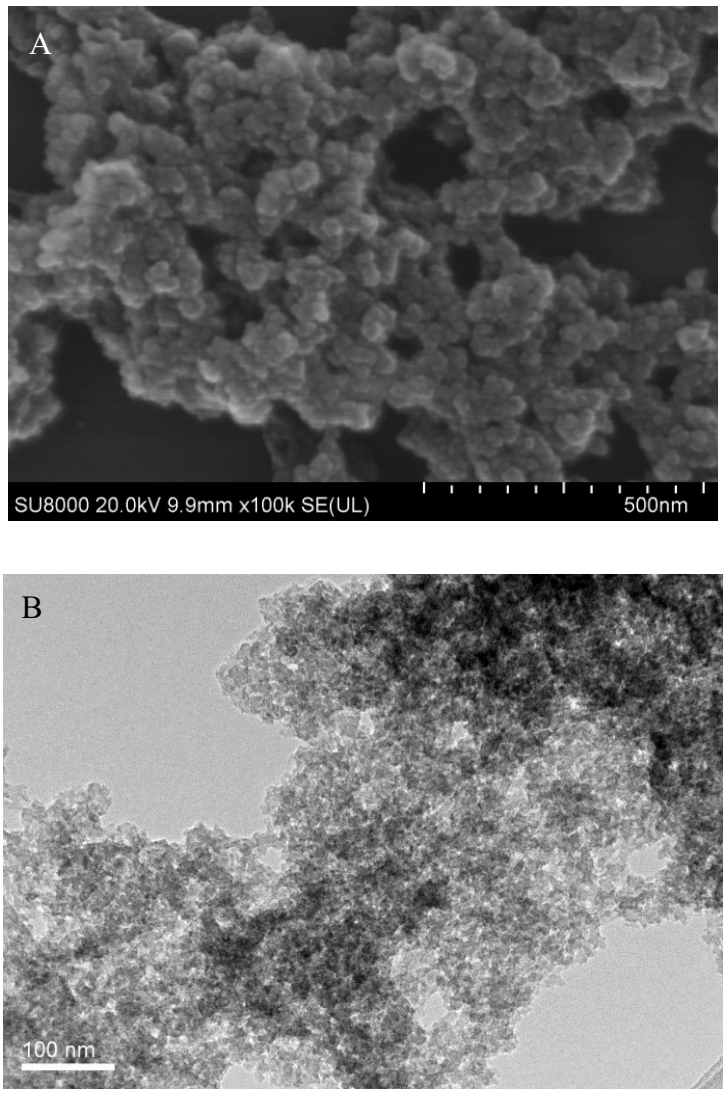

Figure S12. (A) SEM and (B) TEM images of POP-PA-COOH.

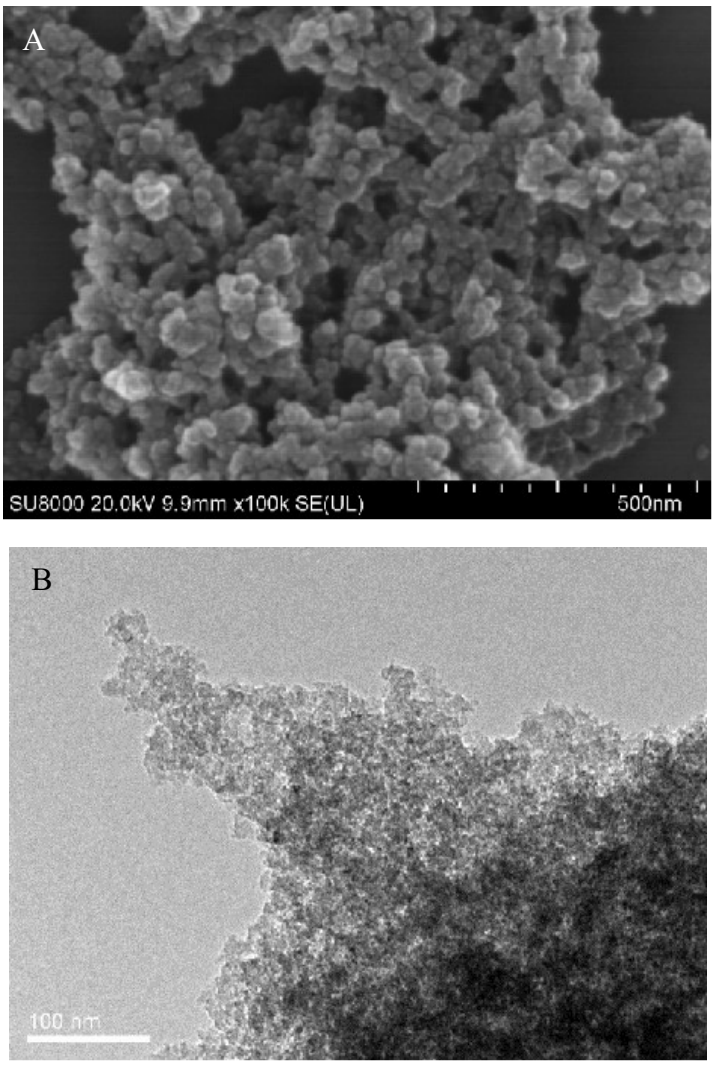

Figure S13. (A) SEM and (B) TEM images of POP-PA-OH.

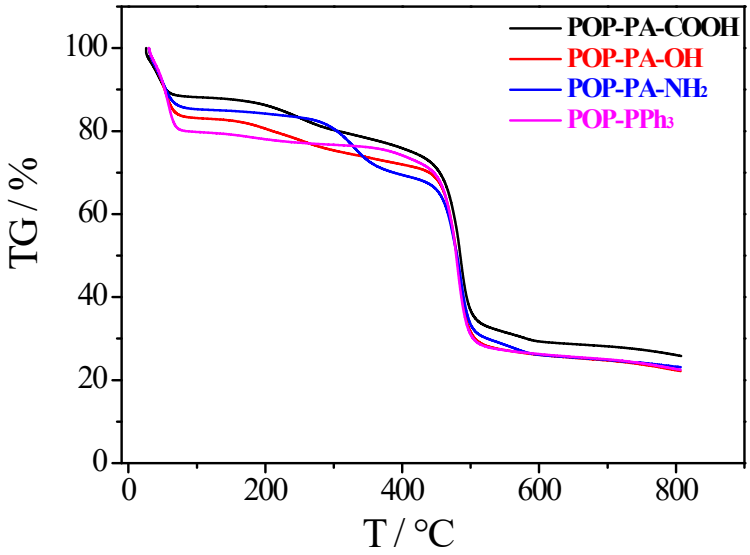

Figure S14. TG curves of POP-PA-NH_2, POP-PA-COOH, POP-PA-OH. The weight loss at below 100 °C is due to the removal of solvent.

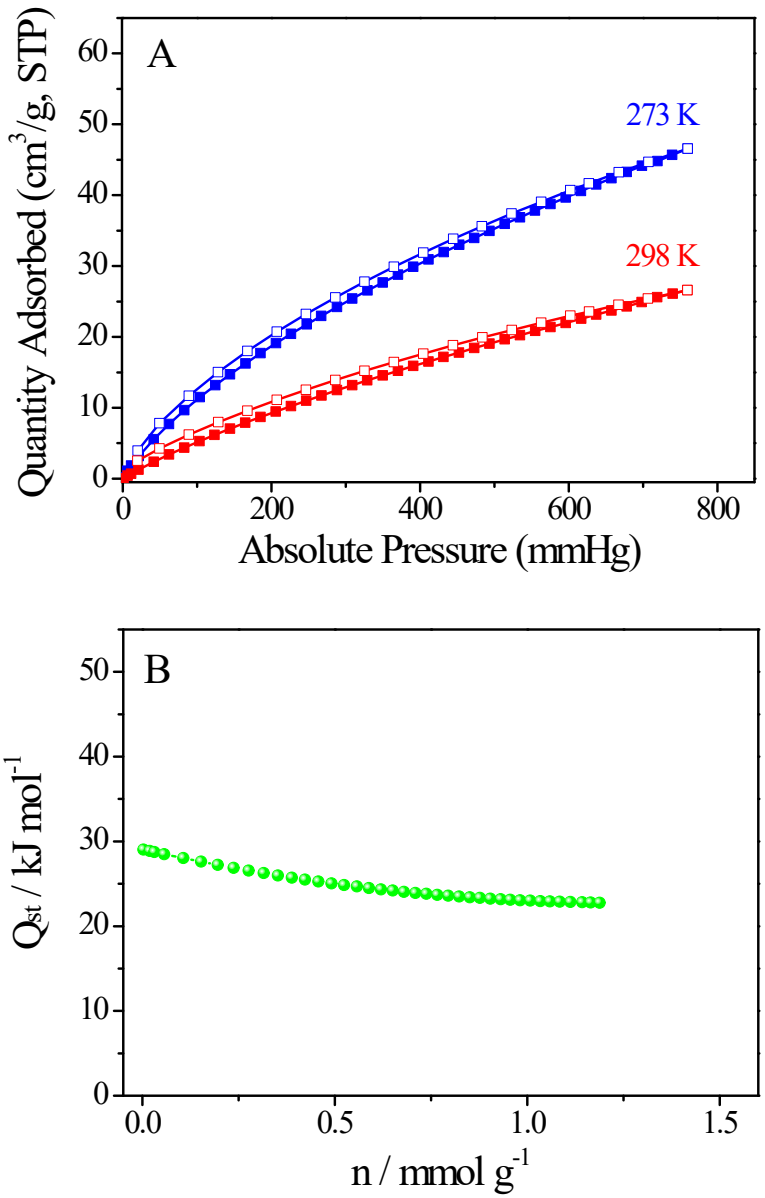

Figure S15. (A) The CO_2 sorption isotherms of POP-PPh_3 measured at different temperatures and (B) the calculated isosteric heat (Q_{st}) by Virial Method.

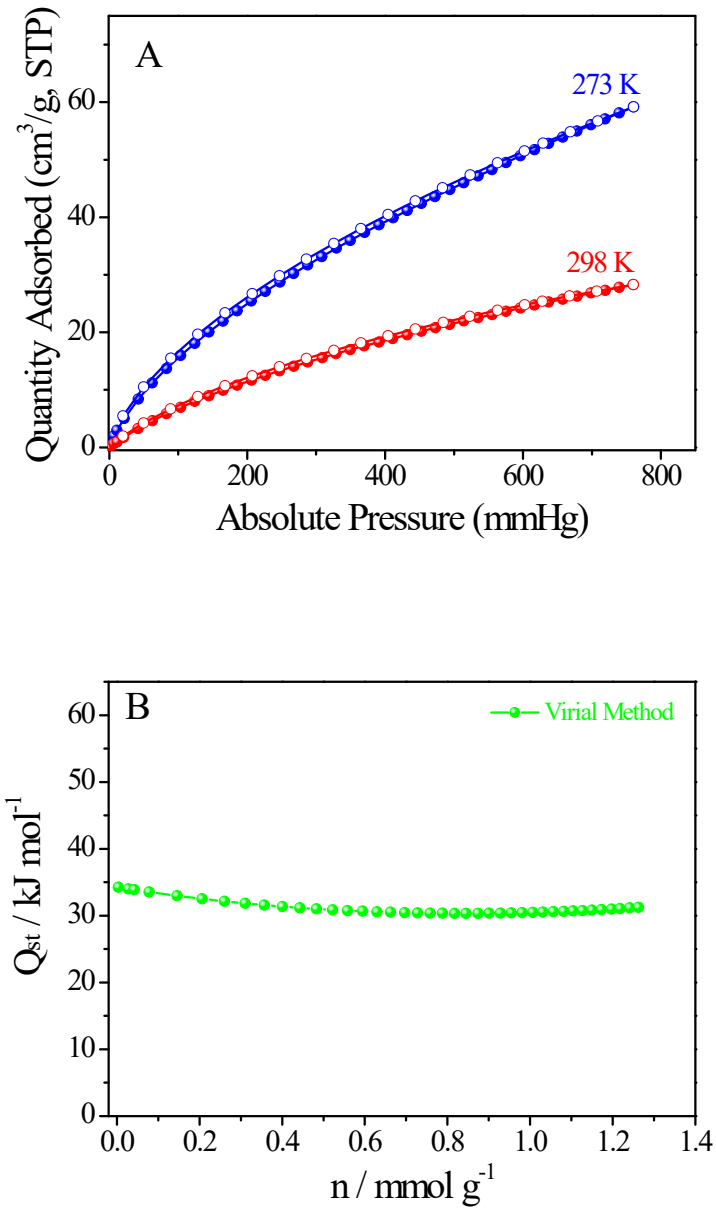

Figure S16. (A) The CO_2 sorption isotherms of POP-PA-NH_2 measured at different temperatures and (B) the calculated isosteric heat (Q_{st}) by Virial Method.

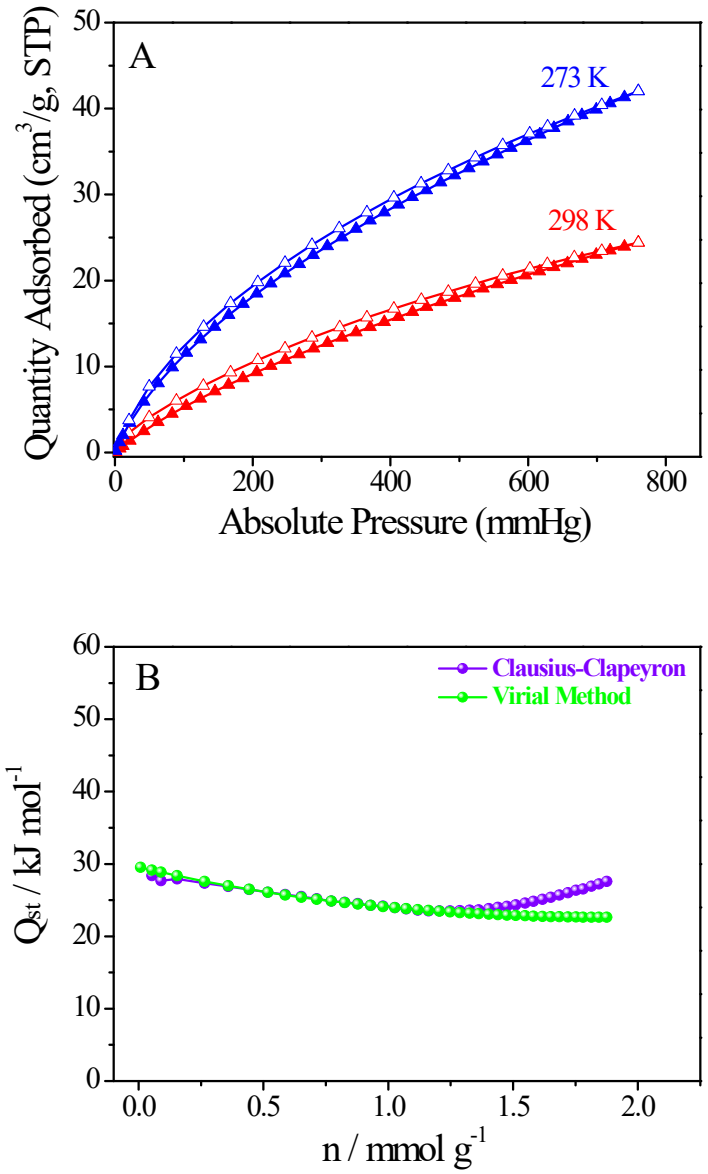

Figure S17. (A) The CO_2 sorption isotherms of POP-PA-COOH measured at different temperatures and (B) the calculated isosteric heat (Q_{st}) by Virial Method and Clausius-Clapeyron Method.

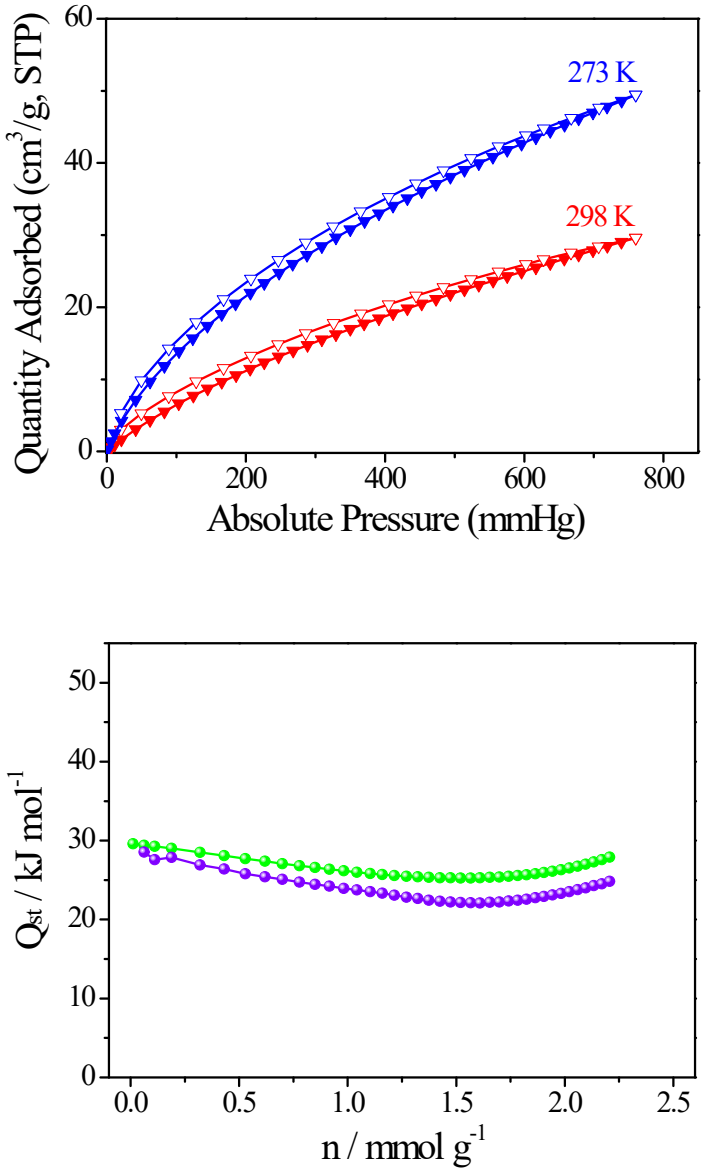

Figure S18. (A) The CO_2 sorption isotherms of POP-PA-OH measured at different temperatures and (B) the calculated isosteric heat (Q_{st}) by Virial Method and Clausius-Clapeyron Method.

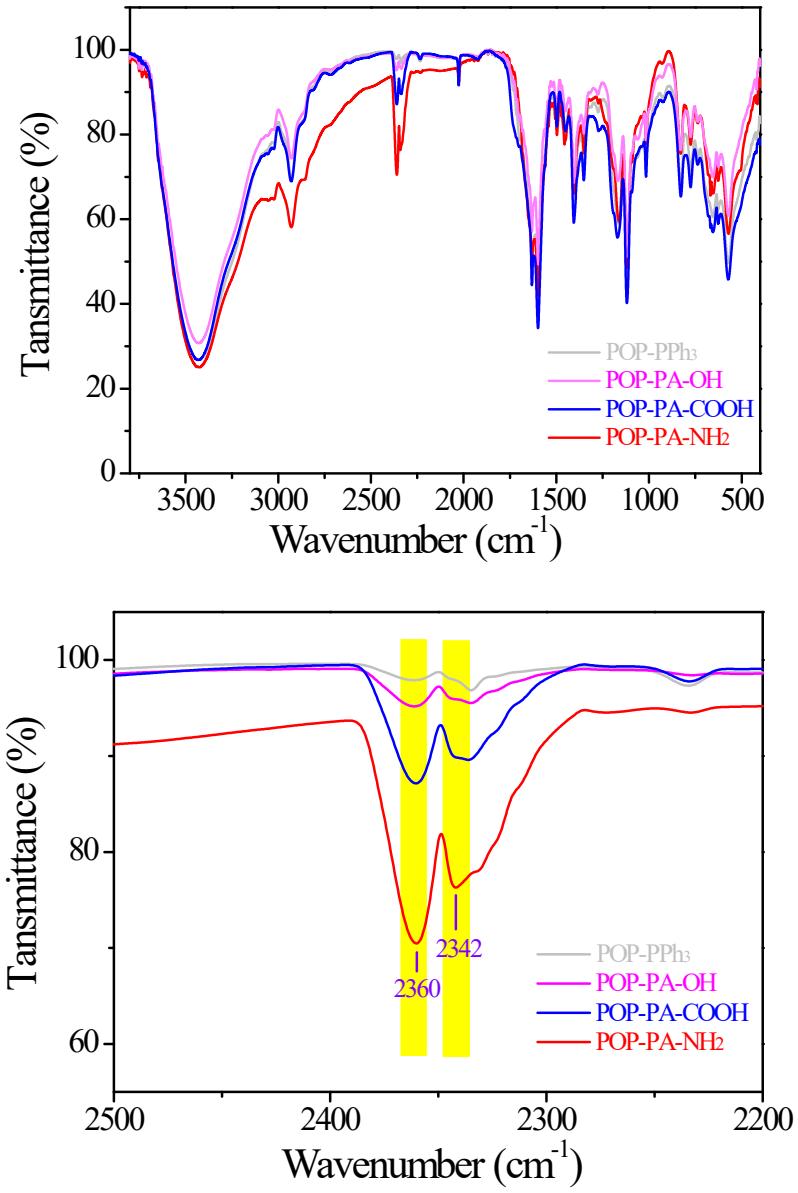

Figure S19. FT-IR spectrum of POP-PPh$_3$, POP-PA-OH, POP-PA-COOH, POP-PA-NH$_2$.

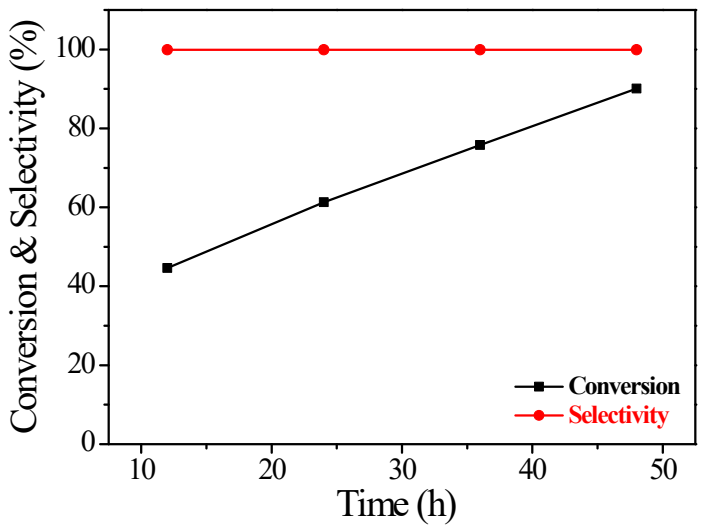

Figure S20. The dependences of conversion and selectivity in the cycloaddition of epichlorohydrin with CO_2 on reaction time over POP-PA-NH_2 under pure CO_2 (1 atm pressure) at 60 °C with catalyst loading of 1.0 mol%.

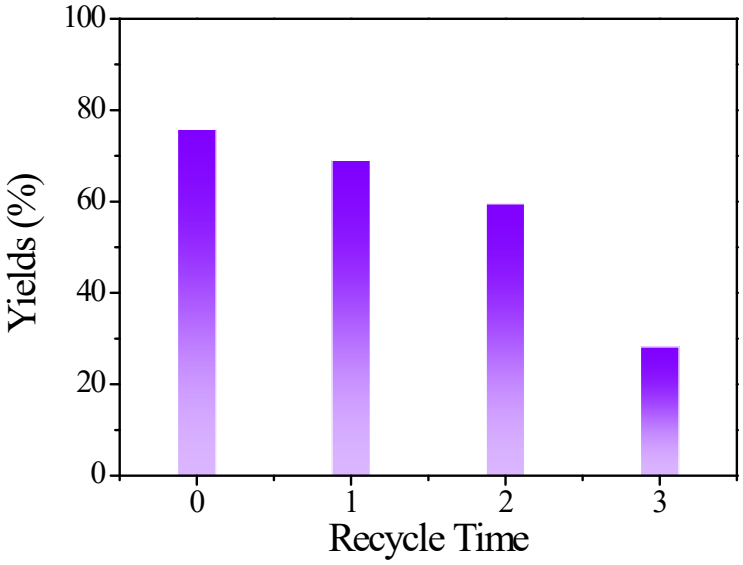

Figure S21. Recycle test of POP-PA-NH_2 in the cycloaddition of CO_2 with epoxides.

Table S1. The textural parameters of various polar groups functionalized hierarchical porous organic polymers.

Polymers	BET (m^2/g)	Pore Volume (cm^3/g)	Element content				
			C (%)	H (%)	N (%)	O (%)	Br (%)
POP-PPh_3	1090	2.31	—	—	—	—	—
POP-PA-NH_2	783	1.43	66.7 (67.3)	6.2 (5.9)	1.2 (3.0)	—	8.3 (10.6)
POP-PA-COOH	754	1.50	65.7 (65.7)	6.2 (5.3)	—	4.13	11.2 (12.9)
POP-PA-OH	847	1.62	66.4 (67.1)	7.2 (5.6)	—	1.64	9.8 (10.7)
POP-PA-Et	774	1.52	67.4 (69.5)	7.3 (5.8)	—	—	8.5 (8.6)

Table S2. CO_2 adsorption performances over various porous materials.

Material	SA_{BET} (m^2/g)	Adsorption capacity (mg/g)		*Q*st (kJ/mol)	Ref.
		273 K	298 K		
POP-PPh_3	1090	91.5	52	29.0	This work
POP-PA-NH_2	783	116	55	31.6	This work
POP-PA-COOH	754	83	48	29.5	This work
POP-PA-OH	847	97	58	29.6	This work
POP-PBnCl-TPPMg-4	411	55	37	28.8	Ref. S1
POP-PBnCl-TPPMg-12	462	82	50.6	31.8	Ref. S1
POP-BPy	1123	130	70	28.0	Ref. S2
POP-TPP	1200	--	58.3	--	Ref. S3
BILP-1	1172	188	131	26.5	Ref. S4
PAF-1	5640	91	--	15.6	Ref.S5
CMP-0	1018	92.4	53.2	--	Ref. S6
TNCMP-2	995	115	64	--	Ref. S6
SMPI-10	112	139	82	--	Ref. S7
TPI-1	809	108	55	34.4	Ref. S8
FJC-1	1726	126	81	20.7	Ref. S9
Co-CMP	965	--	79.3	--	Ref. S10

Table S3. Cycloaddition of CO_2 with various substrates over the POP-PA-NH_2 catalyst[a]

Entry	Epoxide	Product	Temperature (°C)	Time (h)	Conversion (%)[b]	Selectivity (%)[b]
1	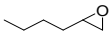		90	48	42.9	99.0
2		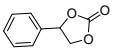	90	48	53.5	99.0
3	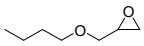	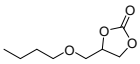	90	48	64.5	99.0
4	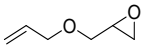	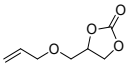	90	48	73.5	99.0
5	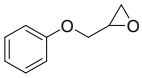	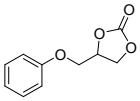	90	48	82.0	99.0

[a]Conditions: substrates (10 mmol), catalyst (1.0 mol% based on the amount of Br^- species) with 1 atm CO_2. [b]Determined by liquid NMR.

Table S4. Catalytic performance of POP-PA-NH_2, POP-PA-COOH, and POP-PA-OH in the cycloaddition of CO_2 with epoxides under low CO_2 concentration (15% v/v with N_2) conditions.[a]

Entry	Catalyst	Time (h)	Conv. (%)	Selectivity (%)
1	POP-PA-NH_2	24	27	>99.0
2	POP-PA-NH_2	48	48.1	>99.0
3	POP-PA-NH_2	72	67.6	>99.0
4	POP-PA-NH_2	96	84.7	>99.0
5	POP-PA-COOH	24	23.5	>99.0
6	POP-PA-COOH	48	39.8	>99.0
7	POP-PA-COOH	72	47.4	>99.0
8	POP-PA-COOH	96	51.2	>99.0
9	POP-PA-OH	24	6.8	>99.0
10	POP-PA-OH	48	13.1	>99.0
11	POP-PA-OH	72	18.8	>99.0
12	POP-PA-OH	96	24.2	>99.0

[a] Conditions: epichlorohydrin (925 mg, 10 mmol), catalyst (0. 48 mol% based on the Br^- species), 60 °C under low CO_2 concentration (15% v/v with N_2) and solvent free conditions.

Supporting References:

[1] Z. Dai, Y. Tang, F. Zhang, Y. Xiong, S. Wang, Q. Sun, L. Wang, X. Meng, L. Zhao, and F.-S. Xiao, *Chin. J. Catal.*, 2021, **42**, 618.

[2] K. P. Divya, S. Sreejith, B. Balakrishna, P. Jayamurthy, P. Anees, A. Ajayaghosh, *Chem. Commun.* **2010**, *46*, 6069-6071.

[3] Z. Dai, † Q. Sun, † X. Liu, L. Guo, J. Li, S. Pan, C. Bian, L. Wang, X. Hu, X. Meng, L. Zhao, F. Deng, and F.-S. Xiao, *ChemSusChem* 2017, 10, 1186-1192.

[4] Z. Dai, Q. Sun, X. Liu, C. Bian, Q. Wu, S. Pan, L. Wang, X. Meng, F. Deng, F.-S. Xiao, *J. Catal.* **2016**, 338, 202-209.

[5] M. G. Rabbani, H. M. El-Kaderi, *Chem. Mater.* **2011**, *23*, 1650-1653.

[6] T. Ben, Y. Li, L. Zhu, D. Zhang, D. Cao, Z. Xiang, X. Yao, S. Qiu, *Energy Environ. Sci.* **2012**, *5*, 8370-8376.

[7] S. J. Ren, R. Dawson, A. Laybourn, J. X. Jiang, Y. Khimyak, D. J. Adams, A. I. Cooper, *Polym. Chem.* **2012**, *3*, 928-934.

[8] Y. Yang, Q. Zhang, Z. Zhang and S. Zhang, *J. Mater. Chem. A* **2013**, *1*, 10368-10374.

[9] M. R. Liebl, J. Senker, *Chem. Mater.* **2013**, *25*, 970-980.

[10] Y. Huang, Z. Lin, H. Fu, F. Wang, M. Shen, X. Wang, R. Cao, *ChemSusChem* **2014**, *7*, 2647-2653.

[11] Y. Xie, T.-T. Wang, X.-H. Liu, K. Zou, W.-Q. Deng, *Nat. Commun.* **2013**, *4*, 1960.